Origin of Polychromism of *Cis* Square-Planar Platinum(II) Complexes: Comparison of Two Forms of [Pt(2,2'-bpy)(Cl)2]

R. H. Herber,[*,†] **M. Croft,**[‡] **M. J. Coyer,**[†] **B. Bilash,**[‡] **and A. Sahiner**[‡]

Departments of Chemistry and Physics, Rutgers University, New Brunswick, New Jersey 08903

Received October 19, 1993[®]

Single crystals of the yellow form of [Pt(2,2'-bpy)(Cl)2] have been prepared, and the crystal structure is compared to that of the Pd(II) homologue reported earlier. The yellow and red modifications of the title compound are compared by FTIR, UV/vis, EXAFS, and hydration studies. The major differences in the two forms arise from differences in the stacking mode of the monomers in the solid-state lattice, with significantly different Pt–Pt distances being observed in the yellow (4.435(1) Å) and red (3.45 Å) complexes. As expected from the similarity of the yellow forms of the Pt(II) complex to the corresponding Pd(II) complex, two inequivalent Pt–Cl distances are noted, in contrast to the architecture of the red form. In the latter, a pseudo-2-fold symmetry axis is preserved in the stacked array, while this symmetry element is absent in the yellow solid owing to a non-2-fold rotation around the Pt–Pt chain axis in the yellow form. The differences in the Pt–Pt scattering maxima extracted from the EXAFS results are in consonance with the crystallographic data.

Introduction

Motivated in part by the antitumor activity of *cis*-Platin, there has been a great deal of interest expressed in the recent chemical literature about the chemical and physical properties of related square-planar Pt(II) complexes, in which two labile ligands occupy *cis* positions in the coordination environment of the metal atom. In particular, the title complex has been reported to exist in several different forms. Morgan and Burstall[1a] reported two modifications (α and β), both of which are described as light yellow, but in a second study[1b] describe in detail the conversion of the yellow form to a red form by treatment of the former with concentrated HCl. In addition, these authors describe an intermediate dihydrate which can be interconverted to the red or yellow form and whose chemical reaction properties are identical to those of anhydrous forms.

The crystal structure of the red form of [Pt(2,2'-bpy)(Cl)2], hereafter referred to as the R form, was reported by Osborn and Rogers,[2] who stated that the crystal structure of the yellow form, hereafter referred to as the Y form, "...is currently under study in this laboratory...", but a definitive structural study of the latter was not reported by them. The crystal structure of [Pd(2,2'-bpy)(Cl)2], which is isomorphous with the Y form of the title compound has been reported by Canty et al.[3] A significant structural feature of the R form noted by Osborn and Rogers[2] relates to the "staggered" arrangement of molecules in adjacent layers, with a Pt–Pt distance of 3.45 Å and an inclination of 4.7° of the coordination planes. A detailed spectroscopic study of both the Y and R forms was reported by Bielli et al.,[4] who first suggested that the difference between the two forms was the stacking arrangement of the metal atoms in the R form, contrasted with the "monomeric" structure of the Y form. Following the earlier observation by Morgan and Burstall,[1b] Bielli et al. effected conversion of the Y form to the R form by heating the former

in pyridine and quenching the resulting reaction by the addition of CCl4, although this procedure was noted to give rise to a mixture of the two forms, depending on the details of the quenching process.

In the present study, the detailed structural differences between the Y form and the R form have been reinvestigated, and the interpretation of X-ray diffraction, EXAFS, hydration kinetic, and vibrational spectroscopic data has afforded a clearer understanding of the origin of polychromism in this compound.

Experimental Section

(a) Synthesis. The Y form of the title complex was prepared in ca. 90% yield by the method of Morgan and Burstal and of Kumar et al.[1b] Anal. Found (calcd) for [Pt(2,2'-bpy)(Cl)2]: C, 28.44 (28.45); H, 1.89 (1.91); N, 6.51 (6.64). The Y form is soluble in both hot dmso and *N*-methylpyrrolidone, which on cooling yield yellow crystals with IR absorbances identical to those of the starting solid. Conversion to the R form was effected by dissolving the Y form in pyridine to which had been added a small amount of water, heating this solution in an oil bath to 120 °C until the volume was reduced to about 25%, filtering the resulting red solid from the hot solution, washing the residue with EtOH, and drying the product over P2O5 at room temperature. Yield: ca. 60%. Anal. Found: C, 28.82; H, 1.83; N, 6.59. Dissolution of the R form in dmso or *N*-methylpyrrolidone gave rise to a yellow solution from which the Y form could be recovered at room temperature. Finally, in this context, it is worth noting that this polychromic conversion is not observed (under similar conditions) for the corresponding Pd complex,[4] for [Pt(1,10-phen)(Cl)2], or for the bis(chloro) complexes of Pt with ring-substituted bpy or phen groups.[2,5] Diffraction-suitable single crystals of the Y form can be obtained from a slowly evaporating solution of the title compound in *N*-methylpyrrolidone and are stable indefinitely at room temperature.

(b) Infrared Characterization. Midrange infrared data were obtained on ca. 1% by weight samples in KBr, using a Mattson Cygnus 100 FTIR spectrometer in transmission geometry. Typically, 64 sample scans at 2-cm⁻¹ resolution were coadded and ratioed to a similar KBr blank background. Detailed data comparisons were effected using the GRAMS-I software (Spectracalc Co.). Far-IR data were acquired using a Perkin-Elmer System 2000 spectrometer at 4-cm⁻¹ resolution in conjunction with a far-IR DTGS detector. A diamond-anvil press was used to disperse the samples without admixture of another medium (e.g. Nujol). A total of 200 sample scans were taken on each sample.

(c) UV/Vis Characterization. Electronic excitation spectra were acquired on samples of the Y- and R-form complexes dispersed in Kel-F stopcock grease and supported on pressed KBr disks, in conjunction with an Aviv Model 14DS spectrometer over the range $250 < \nu < 700$ nm (450 data points).

† Department of Chemistry.
‡ Department of Physics.
® Abstract published in *Advance ACS Abstracts*, May 1, 1994.
(1) (a) Morgan, G. T.; Burstall, F. H. *Indian J. Chem.* **1933**, (see *Chem. Abstr.* **1933**, *27*, 5330). (b) Morgan, G. T.; Burstall, F. H. *J. Chem. Soc.* **1934**, 965. Kumar, L.; Puthraya, K. H.; Srivastava, T. S. *Inorg. Chim. Acta* **1984**, *86*, 173.
(2) Osborn, R. S.; Rogers, D. *J. Chem. Soc., Dalton Trans.* **1974**, 1002.
(3) Canty, A. J.; Skelton, B. W.; Traill, P. R.; White, A. H. *Aust. J. Chem.* **1992**, *45*, 417.
(4) Bielli, E.; Gidney, P. M.; Gillard, R. D.; Heaton, B. T. *J. Chem. Soc., Dalton Trans.* **1974**, 2133.

(5) Herber, R. H. Unpublished results.
(6) G. Sheldrick, XRD, Siemens, Madison, WI.
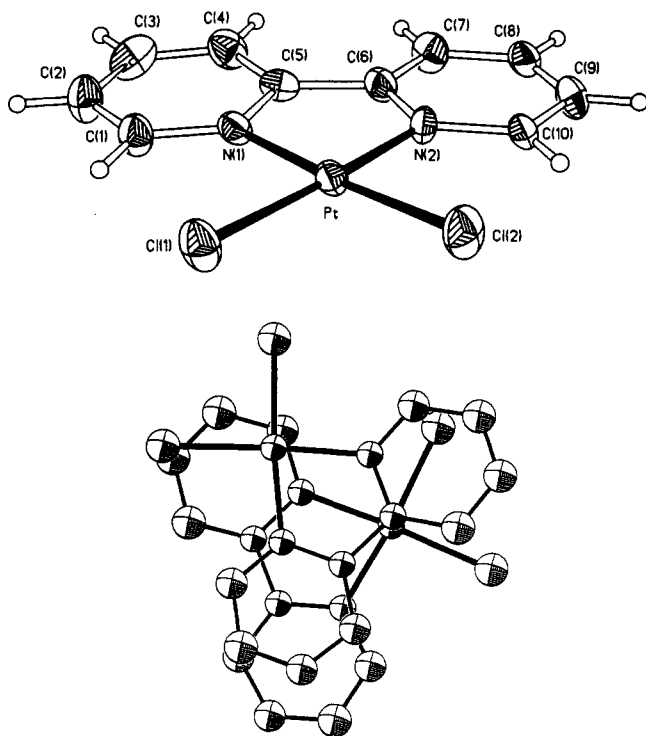
Figure 1. Top: ORTEP representation of the title compound, showing the atomic numbering scheme, drawn with 35% thermal ellipsoids. Bottom: Molecular stacking of the molecules in the Y form of the title compound.

Table 1. Summary of Bond Angles (deg) and Bond Distances (Å) for the Two Forms of [Pt(2,2'-bpy)(Cl)₂] Discussed in the Text[a]

param	Y form[18]	R form[2]
Pt–Cl(1)	2.281(4)	
Pt–Cl(2)	2.300(3)	
Pt–N(1)	2.006(10)	2.001(6)
Pt–N(2)	2.011(10)	
C(5)–C(6)	1.462(17)	1.51(3)
Cl(1)–Pt–Cl(2)	89.1(1)	88(1)
Cl(1)–Pt–N(1)	94.3(3)	96(1)
Cl(2)–Pt–N(1)	175.9(3)	[184][b]
Cl(1)–Pt–N(2)	174.7(3)	[184]
Cl(2)–Pt–N(2)	96.0(3)	96(1)
N(1)–Pt–N(2)		80(1)
Pt–Pt	4.435	3.45
sepn of mol planes, Å		3.40
inclin of Pt–Pt axis, deg		4.7

[a] The numbering scheme reported for the R form in ref 2 has been changed to be consistent with that adopted for the Y form in the present study. [b] Bracketed values calculated from data in ref 3.

(d) EXAFS Studies. The extended X-ray absorption fine structure studies were carried out as described earlier,[7,8] in the absorption mode on beam line X-19A at the Brookhaven National Synchrotron Light Source. Multiple absorption coefficient scans over a range of 1000 eV above the Pt L_3 edge were summed to obtain spectra of sufficient quality for analysis. A continuous-flow nitrogen cryostat was used to effect cooling (110 K) for all of the EXAFS measurements. Data analysis was performed using a modified version of the University of Washington program.[9] The standards used in the fitting routines were generated via a single-scattering program (FEFF) also developed at the University of Washington.[10]

(e) Hydration Studies. Time-dependent weight-gain studies were carried out using a Mettler H51AR microbalance inside a Labconco 5004/5 inert-atmosphere glovebox. The relative humidity in this environment was controlled using saturated salt solutions and monitored with a Fisher Scientific Co. digital relative humidity/temperature indicator. In a typical experiment, samples of the anhydrous solids (previously stored over P_2O_5/vacuum or at 85/°C/vacuum) were introduced in sealed ampules into the glovebox, transferred to the microbalance, and time, temperature, humidity, and weight data were recorded at intervals of 2 min to 2 h, as appropriate.

Results and Discussion

IR Results. The analytical data reported above indicate clearly that the differences in the two modifications of the title compound are not due to differences in hydration stoichiometry. Moreover, the time-dependent weight gain studies showed that, at a relative humidity level as high as 70%, neither the Y form nor the R form absorbs water to any experimentally significant extent at room temperature. In a typical experiment, the weight gain observed for the Y form was equivalent to 0.041 ± 0.084 water molecule

per formula unit in 3.75 h and that for the R form was 0.010 ± 0.010 in 6.5 h. This is in good agreement with the earlier results[11] obtained for the corresponding cyanide complexes, in which the hydration stoichiometry was strongly dependent on the nature of the diamine ligand coordinated to the metal center but in which the unsubstituted bipyridyl complex showed a similar inertness with respect to H_2O absorption.

The midrange IR data for the two forms of the title compound are essentially indistinguishable from each other—the band centers of the seven most intense bands in the range 2000 < ν < 480 agree with each other within ±0.5 cm⁻¹, although, as expected, there are significant differences between these and the corresponding bands of the free ligand. A diagnostic difference in the Y and R forms is that the sharp band at 1313.4 cm⁻¹ for the former is split into a doublet at 1320.2 and 1315.4 cm⁻¹ for the latter. Similarly, the doublet at 1128.3 and 1112.9 cm⁻¹ for the Y form is accompanied by an additional (weak) band at 1118.7 cm⁻¹ for the R form. Finally, the intensity of the band at 737.7 cm⁻¹ (presumably due to a symmetric C–H bending motion) is noticeably more intense for the R form than for the Y-form. These results are understood on the basis of essentially no significant intramolecular change accompanying the Y to R transformation.

In a completely analogous manner, the far-IR data show little significant differences between the Y- and R-form complexes, a fact which had been noted earlier by Bielli *et al.*[4] A medium strong absorbance at 414 cm⁻¹ for the Y form is red-shifted by 6.6 cm⁻¹ for the R form. In addition, there is a weak band at 547 cm⁻¹ for the former which is not observed for the latter, and a weak band at 127 cm⁻¹ for the R form appears to be absent for the Y homologue. Following the earlier assignments of Strukl and Walter[12] and of Walton,[13] Bielli *et al.* assign the two Pt–Cl vibrations to the observed bands at 348 and 335 cm⁻¹ for the Y form and note the presence of a single absorbance at 335 cm⁻¹ for the R form. Similarly, Cooper *et al.*[14] in their study of [Pt-(bpy)Cl(Imn)] have noted a band at 335 cm⁻¹ and assigned this to the Pt–Cl stretching mode. In the present study, both the R and the Y form show an absorbance maximum at 337.1 ± 0.1 cm⁻¹, and this can be associated with the Pt–Cl bond of 2.300(3) (2.306(2)) Å (see Table 2). For the R-form, this band is quite sharp. Significantly, in terms of the X-ray crystallographic data (*vide infra*), the Y form, which evidences two distinct Pt–Cl bond lengths, also shows a shoulder at ca. 350 cm⁻¹. The observation

(7) Coyer, M. J.; Croft, M.; Chen, J.; Herber, R. H. *Inorg. Chem.* **1992**, *31*, 1752.

(8) Coyer, M. J.; Herber, R. H.; Chen, J.; Croft, M.; Szu, S. P. *Inorg. Chem.* **1994**, *33*, 716.

(9) University of Washington Program for EXAFS Data Analysis. See also: Kincaid, B.; Shulman, R. In *Advances in Inorganic Biochemistry*; Parnall, D. W., Wilkins, R. G., Eds.; Elsevier: Amsterdam, 1980; Vol. 2, p 303 and references therein.

(10) Rehr, J. J.; Mustre de Leon, J.; Zabinsky, S. I.; Albers, R. C. *J. Am. Chem. Soc.* **1991**, *113*, 5135. Mustre de Leon, J.; Rehr, J. J.; Zabinsky, S. I.; Albers, R. C. *Phys. Rev.* **1991**, *B44*, 4146.

(11) Shih, K.-C.; Herber, R. H. *Inorg. Chem.* **1992**, *31*, 5444.

(12) Strukl, J. S.; Walter, J. L. *Spectrochim. Acta* **1971**, *27A*, 223.

(13) Walton, R. A. *Can. J. Chem.* **1966**, *44*, 1480.

(14) Cooper, D.; Yaniuk, W.; McPartlin, M. *J. Organomet. Chem.* **1979**, *166*, 241.

Table 2. Comparison of Selected Bond Distances (Å) and Bond Angles (deg) in Pt(II) and Pt(IV) Complexes

compd	Pt–N	C–C′ [a]	N(1)–Pt–N(2)	Pt–Cl	ref
[Pt(bpy)(Cl)₂]–Y	2.006(10)	1.462(17)	80.6(4)	2.281(4)	18
	2.011(10)			2.300(3)	
[Pt(bpy)(Cl)₂]–R	2.001(6)	1.51(3)	80(1)	2.306(2)	2
[Pt(bpy)(CN)₂]	2.00(1)	1.50(2)	84.3(8)		20
[Pt(bpy)(NCO)₂]	1.99(2)	1.57(4)	76(2)		21
	2.00(5)				
[Pt(dmbpy)(NCO)₂][b]	1.96(2)	1.47(3)	82.3(6)		22
	2.03(1)				
[Pt^IV(bpy)(Cl)₄]	2.038(8)	1.480(15)	81.3(4)	2.320(3)	23
	2.044(9)		89.1(1)	2.316(3)	
				2.306(3)	
				2.307(3)	
[Pt(bpy)(Imn)Cl]ClO₄[c]	2.07(5)			2.33(2)	24
	2.25(4)				
	2.15(5)				
[Pt(bpy)₂](TCNQ)₂[d]	2.00(1)	1.47(2)	78.3(4)		25
	2.04(1)				
[Pt(bpy)₂](TCNQ)₃[d]	2.02(2)		77(1)		26
[Pt(bpy)₂](NO₃)·2H₂O	2.025(4)	1.486(9)	80.1(2)		27
	2.028(5)	1.465(11)	80.0(2)		
[Pt(bpy)₁.₃(phen)₀.₃](NO₃)·2.03H₂O[e]	2.025(1)	1.431(17)	80.2(4)		27
	2.005(8)	1.475(22)	79.0(5)		
[Pt(phen)₂(Cl)₂][e]	2.033(6)		80.1(3)		26
[Pt(en)(Cl)₂][f]	2.08(3)	1.42(9)	73(2)	2.288(8)	28
[Pt(dmen)(Cl)₂][g]	2.039(14)	1.47(2)	84.0(5)	2.303(4)	29
	2.067(12)			2.317(4)	

[a] C–C bond distance (Å) of the bridging atoms in bpy and phen. [b] dmbpy = 4,4′-dimethyl-2,2′-bipyridine. [c] Imn = o-isopropenyl-N,N-dimethylaniline. [d] TCNQ = 7,7,8,8-tetracyanoquinodimethane. [e] phen = 1,10-phenanthroline. [f] en = ethylenediamine. [g] dmen = N,N-dimethylethylenediammine.

of two Pt–Cl vibrational modes is consistent with the presence of two (2.303(4) and 2.281(4) Å) Pt–Cl bonds, with both Pt–Cl bonds participating in both vibrations. Notwithstanding these minor differences, it is again concluded that the intramolecular architectures of the two forms appear to be very similar. Finally, it is worth noting that the bands at 175.5, 296, and 387 cm⁻¹ in the IR spectrum of the Y form have an exact analog (within 1 cm⁻¹) in the Raman spectrum of the same compound, as expected from the point-group symmetry of the complex.

UV/Vis Results. The UV/vis spectra of the two forms (in KBr pellets) show absorbances at ∼328 and 396 nm, similar to those reported for related Pt(II) complexes without other chromophoric groups. Careful subtraction of the Kel-F mulled samples shows the presence of a broad absorbance, centered at ∼550 nm in the R-form complex spectrum, in contrast to the Y-form spectrum. A band at essentially the same frequency has been observed by Zhou and Kostic[15] for the red (stacked) form of K[Pt(dipic)Cl] and is characterized as diagnostic of one-dimensional stacking in the solid state. These authors have assigned the absorbances in the 328–355-nm range as being due to a Pt(II) → pyridine MLCT transition. Using a dispersive spectrometer (with its associated calibration difficulties) Bielli *et al.*[4] have reported absorbances at 520 and 458 nm for the R form. The former is polarized along the needle axis (i.e., perpendicular to the molecular planes) and they ascribe the red color of the R form as being due primarily to this 520-nm absorbance. Gidney *et al.*[16] and others[17] have similarly discussed the UV/vis spectra of related Pt complexes and also ascribe bands in the 467–520-nm range as being responsible for the perceived deeper color of these solids, as compared to the monomeric entities present in the (yellow) solutions.

Comparison of X-ray Data. The atom-numbering scheme is shown in Figure 1 (top) and the molecular stacking of the Y form in Figure 1 (bottom). A comparison of the single-crystal

diffraction studies of the R form of the title compound[2] and of the yellow form of the Pd homologue[3,18] is summarized in Table 1. Selected bond angles and bond distances of a number of Pt(II) and Pt(IV) complexes are compared in Table 2. Two major differences are immediately apparent. The Pt–Pt distances are quite different, and (concomitantly) the arrangement of molecules in adjacent layers has changed from a staggered (180°) in the Y form to a rotated orientation in the R form, in which the layer stacking is not perpendicular to the Pt–Pt axis, as it is in the Y form. Not surprisingly, in the latter arrangement (in which there is no pseudo-2-fold axis along the metal–metal direction) there are two inequivalent Pt–Cl distances (2.281(4) and 2.300(3) Å) compared to the value of 2.306(2) Å reported for the R form. In the Pd complex,[3] the corresponding Pd–Cl distances are 2.317 and 2.277 Å. Similarly, the single Pt–N distance of 2.001(6) Å in the R form is to be compared to the 2.006(10 and 2.011(10) Å distances observed in the Y form. Finally, the (calculated) Cl–Pt–N angle of 184° in the R form is to be compared to the significantly smaller values of 175.9(3) and 174.7(3)° in the Y form. Thus, it is apparent, that the R form, obtained from the high-temperature treatment of the Y form, accomodates a Pt–Pt stacking arrangement with significantly larger metal–metal interaction than is present in the latter. Room-temperature solution of the R form and subsequent solvent removal cause the re-formation of the yellow form with its essentially monomeric molecular unit structure.

EXAFS Results. Confirmation of both the structural similarities and differences between the Y and R forms of the title compound can be extracted from the EXAFS data. EXAFS analysis is based on the oscillations of the X-ray absorption coefficient, $\chi(k)$ (about its average), as a function of the photoelectron wavenumber (k). Here $\chi(k)$ is normalized to the absorption coefficient jump at the edge, above which the oscillations occur.[7,9,19] The Fourier transforms of the weighted

(15) Zhou, X.-Y.; Kostic, N. M. *Inorg. Chem.* **1988**, *27*, 4402.
(16) Gidney, P. M.; Gillard, R. D.; Heaton, B. T. *J. Chem. Soc., Dalton Trans.* **1973**, 132.
(17) Patterson, H. H.; Tewksbury, J. C.; Martin, M.; Krogh-Jespersen, M.-B.; LoMenzo, J.; Hooper, H. O.; Viswanath, A. K. *Inorg. Chem.* **1981**, *20*, 2297. Houlding, V. H.; Miskowsky, V. M. *Coord. Chem. Rev.* **1991**, *111*, 145 and references therein.

(18) An analysis of the crystallographic data for the yellow Pt complex, based on the data of ref 3, has been generously made available to us by Prof. A. L. Rheingold (personal communication).
(19) Lee, P. A.; Citrin, P.; Eisenberger, P.; Kincaid, B. *Rev. Mod. Phys.* **1981**, *53*, 769 and references therein.
(20) Che, C.-H.; He, L.-Y.; Poon, C.-K.; T. C. W. *Inorg. Chem.* **1989**, *28*, 3081.
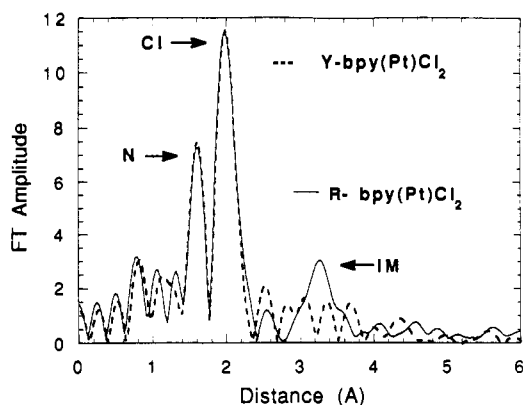
Figure 2. FT spectra of PtL_3 EXAFS data of the R form (solid line) and the Y form (dashed line) of $[Pt(2,2'-bpy)(Cl)_2]$. The nearest neighbor N and Cl featrues, common to both forms, are labeled. In addition, the feature labeled IM, found only for the R form, is associated with the intermolecular correlations present in this crystallographically distinct structure.
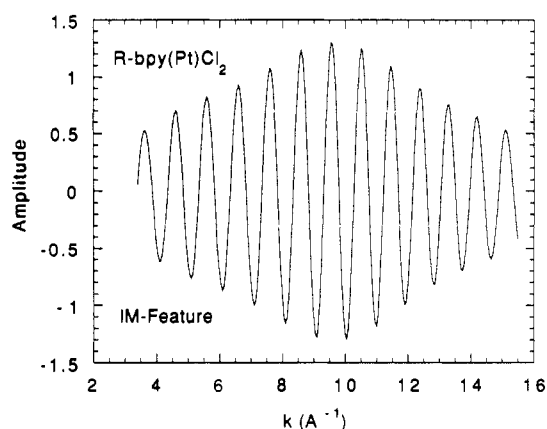
Figure 3. Back-transform to k-space of the IM feature in Figure 2. The "window" for this back-transform spans $2.79 < R < 3.75$ Å.

function, $k^3\chi(k)$ (hereafter referred to as FT) above the Pt L_3 edge for the Y and R forms of $[Pt(2,2'-bpy)(Cl)_2]$ are shown in Figure 2.

The two largest features in both FT curves (between 1.5 and 2.6 Å in Figure 2) are associated with backscattering from the two N and two Cl nearest neighbors. It should be noted that these N and Cl features are essentially identical (within the resolution of the EXAFS method) in the Y and R forms, in consonance with the X-ray diffraction results, which show the coordination environment around the metal atom to be essentially the same in the two forms. Using a standard least-squares fitting method,[9,19] the Pt–Cl distance of 2.31 ± 0.015 Å and the Pt–N distance of 1.97 ± 0.015 Å are found common to both the Y and R forms and are in acceptable agreement with the values of 2.281(4) and 2.006(10) Å reported in Table 2. In this work, the error bars on the fitted interatomic separations (r) are determined by the width of the minimum in the set of fitted χ^2 values in a

(21) Coyer, M. J.; Herber, R. H.; Cohen, S. *Inorg. Chim. Acta* **1990**, *175*, 47.
(22) Coyer, M. J.; Herber, R. H.; Cohen, S. *Acta Crystallogr.* **1991**, *C47*, 1376.
(23) Hambley, T. W. *Acta Crystallogr.* **1986**, *42*, 49.
(24) Cooper, M. K.; Yaniuk, D. W.; McPartlin, M. *J. Organomet. Chem.* **1979**, *166*, 241.
(25) Dong, V.; Endres, H.; Keller, H. J.; Moroni, W.; Noethe, D. *Acta Crystallogr.* **1977**, *B33*, 2428.
(26) Hazell, A.; Mukhopadhyay, A. *Acta Crystallogr.* **1980**, *B36*, 1647.
(27) Hazell, A.; Simonson, O.; Wernberg, O. *Acta Crystallogr.* **1986**, *C42*, 1707.
(28) Iball, J.; MacDougall, M.; Scrimgeour, S. *Acta Crystallogr.* **1975**, *B31*, 1672.
(29) Melanson, R.; de la Chevrotiere, C.; Rochon, F. D. *Acta Crystallogr.* **1987**, *C43*, 57.

Figure 4. Top: $k^3\chi(k)$ data for the red (R) and yellow (Y) isomorphs of $[Pt(2,2'-bpy)(Cl)_2]$. (Bottom): Difference spectrum $[k^3\chi_{diff}(k)]$ obtained by subtracting the two curves $[k^3\chi_R(k) - k^3\chi_Y(k)]$ in the top figure, with the subscripts indicating the isomorph.

series of fits. This series of fits involves (a) fitting for the best r value for a given relative edge energy difference between the standard and the unknown, (b) stepping the edge energy to establish the χ^2 minimum in this series of fits, and (c) observing the r-parameter deviations across this minimum. The Pt–N and Pt–Cl "standards" used in this fit were calculated using a single-scattering theory.[10] The small variation in these Pt nearest neighbor bond lengths, detected in the X-ray diffraction data, are beyond the resolution limit of the EXAFS technique.

(i) **Intermolecular Correlations.** In view of the weakness of the higher-shell contributions to the EXAFS spectrum, two treatments have been used to extract information on the intermolecular (IM) correlations in these compounds. The first treatment is an analysis of the spectrum of the R form, with a constrained fitting procedure for the IM contributions. The second treatment involves an analysis of the differential spectrum of the two isomorphs.

(ii) **IM Correlations: R-Form Feature Analysis.** In analogy with the previous EXAFS study of the Y and R forms of $[Pt-(2,2'-bpy)(SCN)_2]$,[7] intermolecular stacking (IM) effects should be observable in the range $r > 2.5$ Å for the R form but should be absent for the Y form. In this context, the FT feature (labeled IM in Figure 2 and falling in the range $2.79 < R < 3.75$ Å) is associated with such intermolecular stacking in the R form. The back-transform of this IM feature to k-space is shown graphically in Figure 3.

Two points of difference from the previous study of the IM features in the EXAFS data of the R form of $[Pt(2,2'-bpy)-(SCN)_2]$[7] should be noted. First, the IM–FT feature in the R form of the title compound is weaker than those in the earlier study, suggesting a large Debye–Waller factor reduction in the IM correlation. Second, the envelope of the IM back-transform curve, Figure 3, fails to show the large high-k peak which was taken to be characteristic of the IM Pt–Pt correlation in the thiocyanate complexes (i.e., a high-Z atom such as Pt exhibits a back-transform envelope strongly peaked above 12 Å^{-1} due to its backscattering form factor).[7] This second point is also consistent with a large Debye–Waller factor cutoff in Pt backscattering at large k (i.e. an $\exp(-k^2\sigma^2)$ type cutoff).[19]

Combining the X-ray diffraction results with single-scattering calculations,[10] it is expected that both the adjacent two Pt and the four N atoms bound to them will yield FT features in the 2.79 $< r <$ 3.75 Å window where the IM feature of the R form is observed. The weakness of the IM feature, the possible two-shell contributions to it, and the large Debye–Waller dampening, which washes out the high-k strong Pt signature, make quantitative fitting to this feature difficult. In the present analysis a highly constrained fit has been employed, where the numbers of Pt and N neighbors are fixed at 2 and 4, respectively (as anticipated from the diffraction results), and where the Debye–Waller factors of both atoms are constrained to be equal. Under these limitations, an IM Pt–Pt distance of 3.36 ± 0.02 Å and an IM Pt–N distance of 3.64 ± 0.01 Å are obtained from the fitting process.[9,19] Comparing these values to those derived from the room-temperature X-ray data (Pt–Pt = 3.45 Å and Pt–N = 3.76 Å), it is noted that the EXAFS values are contracted by similar factors (0.971 ± 0.003). This could be a reflection of the thermal contraction of the IM distance on cooling. Moreover, the large Debye–Waller factor referred to above is consistent with a large value of the thermal vibration amplitude and hence with a substantial thermal expansion. The EXAFS fit constraints and limited signal to noise ratio in these data dictate that further study of the thermal expansion effect is required.

(iii) IM-Correlations: Differential Analyses. Motivated by the need to substantiate the IM correlations noted above, and the identity of the large molecular units of the R and Y forms of the title compound, a second-differential EXAFS analysis has also been carried out. The $k^3\chi_R(k)$ and $k^3\chi_Y(k)$ oscillations for the R and Y isomorphs, respectively, are shown in Figure 4 (top). Since the intramolecular contributions to $\chi(k)$ should be identical for the two isomorphs, forming the difference spectrum $k^3\chi_{diff}(k)$ = $k^3\chi_Y(k)$ should lead to a cancellation of these contributions. This difference spectrum has been calculated and is shown in Figure 4 (bottom). The FT of $k^3\chi_{diff}(k)$, over a range spanning the R-form IM feature, is shown in Figure 5 (bottom). [For reference, an expanded view of the R-form FT of $k^3\chi_R(k)$ is shown in Figure 5 (top)].

This substraction procedure significantly reduces the background contribution to the IM feature signal and yields a better defined IM(diff) feature. The back-transform of the IM(diff) feature (using the r-space window indicated in the figure) yields the IM(diff) back-transform [IM(diff)–BT] spectrum shown in Figure 6.

The faster low-k drop-off and movement of the envelope peak to higher k makes the difference spectrum of Figure 6 more amenable to a single-Pt-shell fit than was the R-form IM feature back-transform-analyzed in the previous treatment. Fitting the IM(diff)–BT spectrum to a single Pt shell, over the 7 $< k <$ 15 Å range (where the Pt contribution should dominate), yields a very good fit with R_{Pt} = 3.37 ± 0.01 Å, N_{Pt} = 1.6, and σ^2 = 0.0046. This Pt–Pt distance (R_{Pt}) is in good agreement with the fit results obtained in the R-form treatment, above. The coordination number (N_{Pt}) is also consistent with the earlier fit method, in view of the typically large uncertainty in coordination number and its strong coupling to the Debye–Waller factor uncertainty.
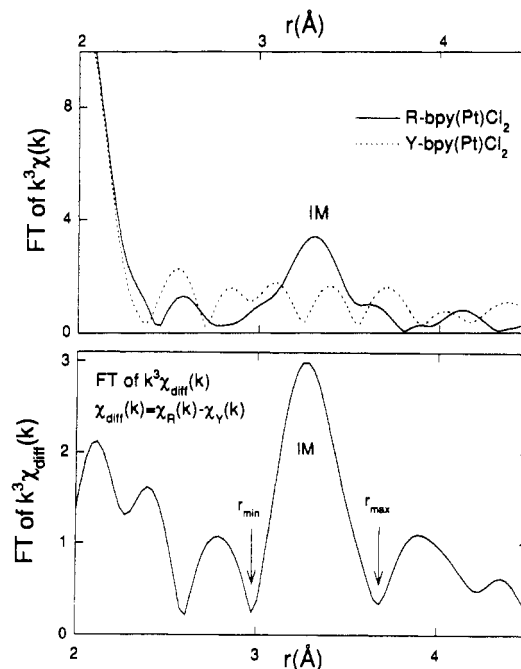
Figure 5. Bottom: Fourier transform of $k^3\chi_{diff}(k)$. The limits for the back Fourier transform (shown in Figure 6) are indicated by arrows. Top: Expanded view of Figure 2 emphasizing the correspondence of the IM feature of the R form and in the difference spectrum, as well as showing the better definition of the IM feature in the latter.
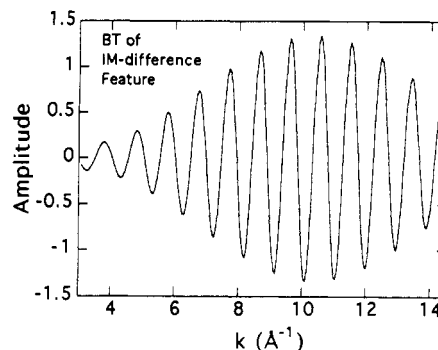
Figure 6. Back-transform spectrum of the IM difference feature shown in Figure 5 (bottom).